

Thermal Diffusivity Mapping of Solids by Scanning Photoacoustic Piezoelectric Technique

Binxing Zhao^{1,2} · Chunming Gao^{1,2} · Laijun Yan¹ · Yafei Wang¹

Received: 8 October 2015 / Accepted: 15 September 2016 / Published online: 17 October 2016
© Springer Science+Business Media New York 2016

Abstract Quantitative thermal diffusivity mapping of solid samples was achieved using the scanning photoacoustic piezoelectric (PAPE) technique. Based on the frequency-domain PAPE theoretical model, the methodology of the scanning PAPE thermal diffusivity mapping is introduced. An experimental setup capable of spatial and frequency scanning was established. Thermal diffusivity mapping of homogeneous and inhomogeneous samples was carried out. The obtained thermal diffusivity images are consistent with the optical images in image contrast and consistent with the reference values in thermal diffusivity. Results show that the scanning PAPE technique is able to determine the thermal diffusivity distribution of solids, hence providing an effective method for thermal diffusivity mapping.

Keywords Inhomogeneous materials · Photoacoustic piezoelectric technique · Thermal diffusivity mapping

This article is part of the selected papers presented at the 18th International Conference on Photoacoustic and Photothermal Phenomena.

✉ Chunming Gao
gaocm@uestc.edu.cn

¹ School of Opto-electronic Information, University of Electronic Science and Technology of China, Chengdu 610054, China

² Center for Robotics, University of Electronic Science and Technology of China, Chengdu 610054, China

1 Introduction

As modern material science is rapidly developing, various new materials have been applied in industry. Thermal properties are among the most important properties of materials. Therefore, the study of thermal properties of materials is necessary. In recent years, several photoacoustic and photothermal methods, such as the photothermal radiometry technique [1–3], the photothermal deflection technique [4, 5] the photothermal displacement technique [6] and the photoacoustic piezoelectric (PAPE) technique [7–12], have been applied to the study of thermal physical properties of materials. Among these studies, it is the average/effective thermal diffusivity that was investigated, while the spatially resolved thermal property imaging is still at the qualitative stage [1–12].

Introduced by Rosencwaig in 1970s, the PAPE technique has been proved to be an effective method for thermal diffusivity determination [7]. In recent years, some revised PAPE theoretical models were developed and applied to thermal diffusivity determination of metals, composite and biological materials [9–12]. In this work, an experimental system for the scanning PAPE thermal diffusivity mapping was developed. Based on the frequency-domain PAPE theoretical model, the thermal diffusivity mapping of solids was studied.

2 Theory

Figure 1 shows the theoretical model under investigation. A periodic heat source is generated inside the sample when illuminated by a periodically modulated laser. As a result, thermoelastic waves are generated and detected by a piezoelectric transducer adhered on the sample back. The detected PA signal is dependent on the thermal diffusivity; therefore, the thermal diffusivity can be extracted through best fitting.

Generally, a sample could be treated as a double-layer model. Assume the layer 1 is thermally thick, so it is the propagation medium of both the thermal and the acoustic waves, while the layer 2 only acts as the acoustic-wave propagation medium. Consequently, the determined thermal diffusivity is that of the layer 1. The sample under consideration is a disk, with a PZT piezoelectric transducer adhered to the back. The thicknesses of the two layers and the transducer are represented as l , H and h , respectively.

Assuming that the thin plate condition is satisfied and the effect of the transducer on the sample vibration can be neglected, the frequency dependence of the PAPE phase signal can be written as [10, 11]

$$\tan \varphi = \frac{2U \sin[a(H+l)] \cosh[a(H+l)] + 2V \cos[a(H+l)] \sinh[a(H+l)] + 4apA' \{ \cos^2[a(H+l)] - \cosh^2[a(H+l)] \} - 3pB' \{ \sin[2a(H+l)] - \sinh[2a(H+l)] \}}{2V \sin[a(H+l)] \cosh[a(H+l)] - 2U \cos[a(H+l)] \sinh[a(H+l)] + 3pB' \{ \sin[2a(H+l)] + \sinh[2a(H+l)] \}} \quad (1)$$

Fig. 1 Theoretical model of the PAPE technique

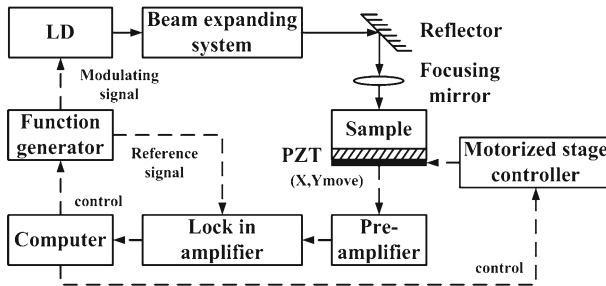
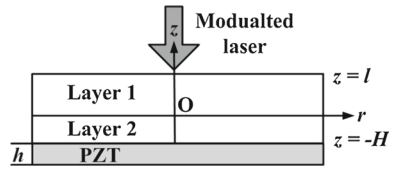


Fig. 2 Schematic of the experimental system

where

$$\begin{cases} A' = H^3 + 3H^2l + 3Hl^2p + l^3p \\ B' = H^2 + 2Hlp + l^2p \\ C' = H^3 - 3Hl^2p - 2l^3p \\ U = 3B'\{1 - (1 - p)[\cos(aH)\cosh(aH) - \sin(aH)\sinh(aH)] \\ \quad - 2aC'(1 - p)\sin(aH)\cosh(aH)\} \\ V = -3B'\{1 - (1 - p)[\cos(aH)\cosh(aH) + \sin(aH)\sinh(aH)] \\ \quad - 2aC'(1 - p)\cos(aH)\sinh(aH)\} \end{cases}$$

with $a = (\omega/2D)^{1/2}$, $p = F_1/F_2$, where $F_{1,2} = E_{1,2}/(1 - \nu_{1,2})$ is a parameter related to the Young's modulus E and the Poisson's ratio ν of the two layers, ω is the laser modulation frequency, and D is the thermal diffusivity of the layer 1.

Equation 1 reflects the relationship between the PAPE signal and the thermal diffusivity, which indicates that the frequency dependence of the PAPE phase signal is determined by D , p and the thicknesses of both layers. Since the thicknesses of the sample and the PZT transducer can be measured, the thermal diffusivity of the layer 1 could be obtained through a three-parameter fitting using Eq. 1. Combined with the spatial scanning, the thermal diffusivity image of the sample can be obtained.

3 Experiments and Results

3.1 Experimental System

Figure 2 shows a schematic of the experimental setup of the scanning PAPE technique. An intensity-modulated 830 nm diode laser with 130 mW power was expanded, reflected and focused on the sample surface. Thermal waves attenuated rapidly below

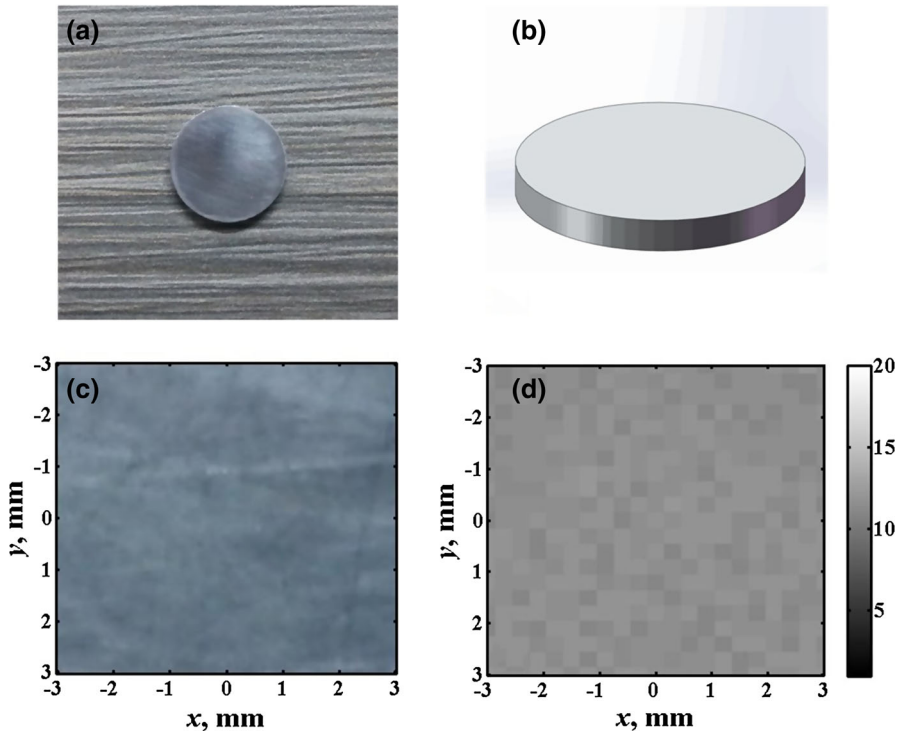


Fig. 3 No. 45 steel sample [(a) sample, (b) geometric diagram, (c) optical image and (d) thermal diffusivity image]

the surface, while acoustic waves were detected by a PZT transducer with 18.2 mm diameter and 0.1 mm thickness, which was adhered to the back surface of the sample by glue. The PAPE signals were measured by a lock-in amplifier. By varying the laser modulation frequency, the frequency-domain PAPE signals were obtained which can be used to determine the thermal diffusivity. A motorized positioning stage controlled by a computer was used for the spatial scanning. The modulation and the reference signals were generated by a function generator.

3.2 Thermal Diffusivity Mapping

Thermal diffusivity mapping of solid samples was carried out by the abovementioned experimental setup. The spatial scanning step was 0.3 mm. The laser modulation frequency was from 11 Hz to 101 Hz, with a frequency scanning step of 5 Hz. The focused laser spot size was 0.2 mm. The mapping resolution was determined by the thermal diffusion length, the laser spot size and the spatial scanning step.

The No. 45 steel sample under investigation and its geometric diagram are shown in Fig. 3a, b. The sample is in disk shape with 17 mm diameter and 1.99 mm thickness. A square area with 6 mm length in the central part of the sample was chosen for mapping.

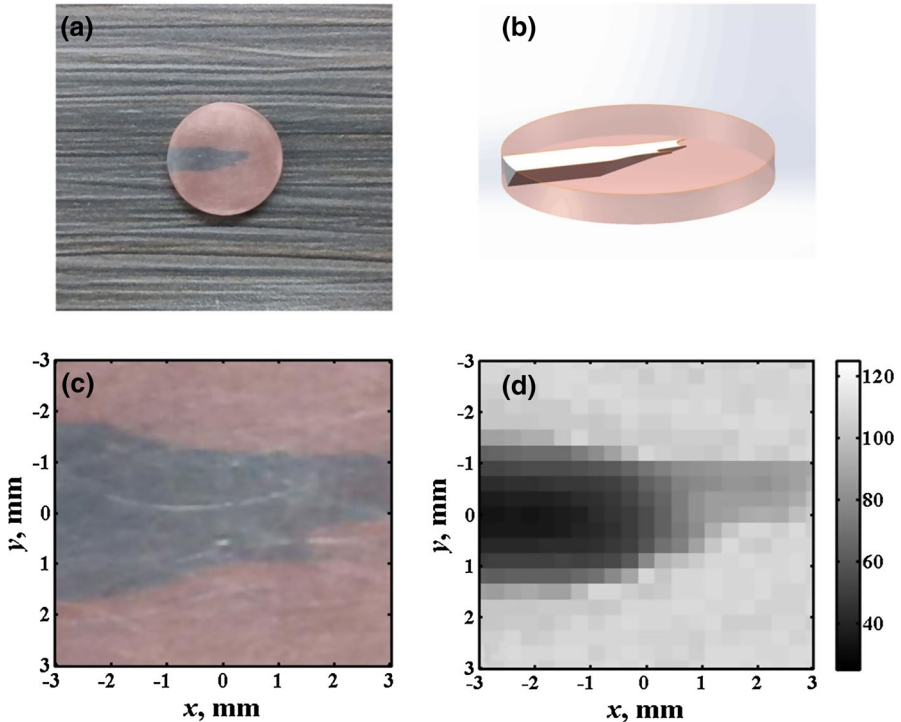


Fig. 4 Inhomogeneous copper/soldering tin composite sample [(a) copper/soldering tin (inverted triangle) sample, (b) stereoscopic perspective, (c) optical image and (d) thermal diffusivity image]

The optical image of the mapped area is shown in Fig. 3c, and the obtained thermal diffusivity image is shown in Fig. 3d.

A copper/soldering tin composite sample and its stereoscopic perspective are shown in Fig. 4a, b. The sample is in disk shape with 17 mm diameter and 1.97 mm thickness. The structure was machined on a copper plate, with an inverted triangle part hollowed out and filled with soldering tin. The filling has a 3 mm width on the top and a 1.5 mm depth within the first 6 mm from the edge of the sample; the next 6 mm extension toward the center has a gradually decreased depth of filling. A square area with 6 mm length in the central part of the sample was chosen for mapping. The optical image of the mapped area is shown in Fig. 4c, and the obtained effective thermal diffusivity image is shown in Fig. 4d. Here the effective thermal diffusivity means the spatially averaged thermal diffusivity within the thermal diffusion region.

The experimental phase-frequency data and the best-fitted theoretical curve of the No. 45 steel sample are shown in Fig. 5a. The calculated thermal diffusivity is $11.87 \text{ mm}^2 \cdot \text{s}^{-1}$, and the measurement uncertainty is about $\pm 5.3\%$. From Fig. 3d, one can see that the sample's thermal diffusivity image is nearly uniform in the tested area. As the thermal diffusion length corresponding to the frequency range used in the experiments is submillimeter, the mapping resolution is also on the order of submillimeter. The calculated thermal diffusivity from Fig. 3d is between $11 \text{ mm}^2 \cdot \text{s}^{-1}$

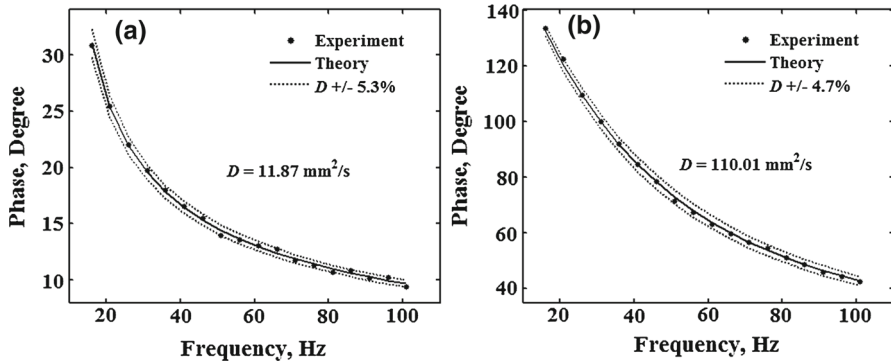


Fig. 5 Experimental phase-frequency data and the best-fitted theoretical curves [(a) the No. 45 steel sample, (b) the copper/tin composite sample]

and $12 \text{ mm}^2 \cdot \text{s}^{-1}$, which is in good agreement with the reference value of steel ($10 \text{ mm}^2 \cdot \text{s}^{-1}$ – $14 \text{ mm}^2 \cdot \text{s}^{-1}$ [13]), with error less than 5 %.

The experimental phase-frequency data and the best-fitted theoretical curve of the copper/ soldering tin composite sample are shown in Fig. 5b. The calculated thermal diffusivity is $110.01 \text{ mm}^2 \cdot \text{s}^{-1}$, and the measurement uncertainty is about $\pm 4.7\%$. From Fig. 4d, one can see that the effective thermal diffusivity image of the sample matches well with the optical image (Fig. 4c). As the thermal diffusion length is less than 1.6 mm, the mapping resolution is better than 2 mm. The determined effective thermal diffusivity in the area with the largest soldering tin-filling duty ratio is $33 \text{ mm}^2 \cdot \text{s}^{-1}$ (the reference value of soldering tin is $30 \text{ mm}^2 \cdot \text{s}^{-1}$, determined by the PAPE technique). From Fig. 4d, it can be observed that the effective thermal diffusivity values gradually increase as the scanning position moves away from the area with the largest soldering tin-filling duty ratio. This feature can be explained by the fact that the determined effective thermal diffusivity is an average value between copper and soldering tin. Since the thermal diffusivity of copper ($117 \text{ mm}^2 \cdot \text{s}^{-1}$ [13]) is larger than that of soldering tin, for positions where the soldering tin-filling duty ratio is smaller, the determined effective thermal diffusivity is larger.

4 Conclusions

Thermal diffusivity mapping of solid samples was achieved by the scanning PAPE technique. The theoretical analysis showed that the PAPE model is applicable to the effective thermal diffusivity mapping. The determined thermal diffusivity values agree well with the reference values, and the contrast of the thermal diffusivity images is consistent with the optical counterpart, which demonstrated the effectiveness of the scanning PAPE technique as an effective thermal diffusivity mapping methodology.

Acknowledgments This work was supported by the National Science Foundation of China (Nos. 61379013 and 61574030) and the Fundamental Research Funds for the Central Universities of China (Nos. ZYGX2012Z006 and ZYGX2015J151).

References

1. S. Pham Tu Quoc, G. Cheymol, A. Semerok, *Rev. Sci. Instrum.* **85**, 054903 (2014)
2. M. Depriester, P. Hus, S. Delenclos, A. Hadj Sahraoui, *Rev. Sci. Instrum.* **78**, 036101 (2007)
3. C.H. Wang, Y. Liu, A. Mandelis, J. Shen, *J. Appl. Phys.* **101**, 083503 (2007)
4. C. Sánchez-Pérez, A. Gutiérrez-Arroyo, N. Alemán-García, *AIP Conf. Proc.* **1494**, 62 (2012)
5. D. Ferizović, L.K. Hussey, Y.S. Huang, M. Muñoz, *Appl. Phys. Lett.* **94**, 131913 (2009)
6. E.H. Lee, K.J. Lee, P.S. Jeon, J. Yoo, *J. Appl. Phys.* **88**, 588 (2000)
7. A. Rosencwaig, A. Gersho, *J. Appl. Phys.* **47**, 64 (1976)
8. W. Jackson, N.M. Amer, *J. Appl. Phys.* **51**, 3343 (1980)
9. I.V. Blonskij, V.A. Tkoryk, M.L. Shendeleva, *J. Appl. Phys.* **79**, 3512 (1996)
10. M.L. Shendeleva, *Proc. SPIE* **3359**, 484 (1998)
11. Q.M. Sun, C.M. Gao, B.X. Zhao, H.B. Rao, *Chin. Phys. B* **19**, 118103 (2010)
12. Q.M. Sun, C.M. Gao, B.X. Zhao, Y.F. Bi, *Int. J. Thermophys.* **31**, 1157 (2010)
13. J.Z. Zhang, *Advanced Heat Transfer* (Science Press, Beijing, 2009)